NASA Technical Paper 1879

Meteoroid Bumper Experiment on Explorer 46

Donald H. Humes

JULY 1981

AUG 1981
RECEIVED
NASA STI FACILITY
ACCESS DEPT.

NASA

N O T I C E

THIS DOCUMENT HAS BEEN REPRODUCED FROM THE BEST COPY FURNISHED US BY THE SPONSORING AGENCY. ALTHOUGH IT IS RECOGNIZED THAT CERTAIN PORTIONS ARE ILLEGIBLE, IT IS BEING RELEASED IN THE INTEREST OF MAKING AVAILABLE AS MUCH INFORMATION AS POSSIBLE.

NATIONAL ADVISORY COMMITTEE FOR AERONAUTICS

TECHNICAL NOTE NO. 523

STRENGTH TESTS OF THIN-WALLED DURALUMIN CYLINDERS IN COMBINED TRANSVERSE SHEAR AND BENDING

By Eugene E. Lundquist

SUMMARY

This report is the fourth of a series presenting the results of strength tests on thin-walled cylinders and truncated cones of circular and elliptic section; it includes the results obtained from combined shear and bending tests on 100 thin-walled duralumin cylinders of circular section with ends clamped to rigid bulkheads. The tests show that as the ratio of moment to shear varies from small to large values the failure changes from a shear to a bending type. In the report a chart is presented that shows the corresponding changes in strength.

INTRODUCTION

As part of an investigation of the strength of stressed-skin structures for aircraft, the National Advisory Committee for Aeronautics in cooperation with the Army Air Corps; the Bureau of Aeronautics, Navy Department; the National Bureau of Standards; and the Bureau of Air Commerce has made an extensive series of tests on thin-walled duralumin cylinders and truncated cones of circular and elliptic section. In these tests the absolute and relative dimensions of the specimens were varied to study the types of failure and to establish useful quantitative data in the following loading conditions: torsion, compression, bending, and combined loading.

The first three reports of this series (references 1, 2, and 3) present the results obtained in the torsion, the compression, and the pure-bending tests of cylinders of circular section. This report presents the results obtained in tests of cylinders of circular section in combined transverse shear and bending.

REPRODUCED BY
NATIONAL TECHNICAL
INFORMATION SERVICE
U.S. DEPARTMENT OF COMMERCE
SPRINGFIELD, VA. 22161

MATERIALS

The duralumin (Al. Co. of Am. 17ST) used in these tests was obtained from the manufacturer in sheet form with nominal thicknesses of 0.011, 0.016, and 0.022 inch. The properties of this material as determined by the National Bureau of Standards from specimens selected at random are given in references 1 and 2. Since all the test cylinders failed by elastic buckling of the walls at stresses considerably below the yield-point stress, the modulus of elasticity E, which was substantially constant for all sheet thicknesses, is the only important property of the material that need be considered. For all cylinders an average value of E (10.4×10^6 pounds per square inch) was used in the analysis of the results.

SPECIMENS

The test specimens were right circular cylinders of 7.5- and 15.0-inch radii with lengths ranging from 3.75 to 15.0 inches. The cylinders were constructed in the following manner. A duralumin sheet was first cut to the dimensions of the developed surface. The sheet was then wrapped about and clamped to end bulkheads. (See figs. 1 to 4, inclusive.) With the cylinder thus assembled, a butt strap 1 inch wide and of the same thickness as the sheet was fitted, drilled, and bolted in place to close the seam. In the assembly of the specimen care was taken to avoid having either a looseness of the skin (soft spots) or wrinkles in the walls when finally constructed.

The end bulkheads, to which the loads were applied, were each constructed of two steel plates one-quarter inch thick separated by a plywood core 1-1/2 inches thick for the bulkheads of 7.5-inch radius and 3-1/2 inches thick for the bulkheads of 15.0-inch radius. These parts were bolted together and turned to the specified outside diameter. Steel bands approximately one-quarter inch thick were used to clamp the duralumin sheet to the bulkheads. These bands were bored to the same diameter as the bulkheads.

APPARATUS AND METHOD

The thickness of each sheet was measured to an estimated precision of ±0.0003 inch at a large number of stations by means of a dial gage mounted in a special jig. In general, the variation in thickness throughout a given sheet was not more than 2 percent of the average thickness. The average thicknesses of the sheets were used in all calculations of radius/thickness ratio and stress.

A photograph of the loading apparatus used in the tests is shown in figure 1. Different ratios of moment to shear were obtained by placing the jack at different distances from the column. In this way it was possible to study the transition from failure by shear at small ratios to failure by bending at large ratios of moment to shear. In all cases the cylinder when mounted for tests had the seam and butt strap located on the extreme-tension fiber. Loads were applied by the jack in increments of about 1 percent of the estimated load at failure.

DISCUSSION OF RESULTS

As far as is known there is no theoretical treatment of the stability of the walls of a thin-walled cylinder in combined transverse shear and bending. Consequently, as an aid to the interpretation of the results of the tests herein considered, some of the important factors will be discussed.

From purely physical considerations it is clear that the magnitude of the shear V and the moment M relative to the size of the cylinder should be considered in the analysis of the test results. Consequently, V, M, and r (where r is the radius of the cylinder) have been combined to form a nondimensional term $\frac{M}{rV}$ that is descriptive of the loading condition. Physically, the term $\frac{M}{rV}$ is the distance from the section under investigation to the resultant shear force in terms of the radius of the cylinder. (See fig. 5.)

$$\frac{M}{rV} = \frac{V\,(d - x)}{rV} = \frac{d - x}{r}$$

If it is assumed that the ordinary beam theory applies, as was done in the analysis of the results of the pure-bending tests on thin-walled cylinders (reference 3), it follows that before buckling occurs the compressive stress on the extreme fiber and the shearing stress at the neutral axis are, respectively

$$f_b = \frac{M}{\pi r^2 t} \tag{1}$$

and

$$f_v = \frac{V}{\pi rt} \tag{2}$$

In these equations t is the thickness of the cylinder wall.

If equation (1) is divided by equation (2) the following relation is obtained:

$$\frac{f_b}{f_v} = \frac{M}{rV} \tag{3}$$

Thus, a particular value of $\frac{M}{rV}$ is descriptive of a definite stress condition as well as a definite loading condition in the same manner that torsion, compression, and pure bending are descriptive of definite stress conditions, and hence definite loading conditions. In the analysis of the results of the tests, the variation of the bending stress at failure with $\frac{M}{rV}$ is studied for each of the following groups of cylinders tested. (For the tabulated data, see tables I and II.)

Group	r	l/r	r/t	Nominal sheet thickness
	Inches			Inch
1	7.5	1.0	323 - 366	0.022
2	7.5	1.0	452 - 490	.016
3	7.5	.5	586 - 670	.011
4	7.5	1.0	625 - 694	.011
5	7.5	2.0	581 - 688	.011
6	15.0	1.0	647 - 746	.022
7	15.0	1.0	932 - 980	.016
8	15.0	1.0	1293 - 1455	.011

From figure 2 it will be noted that failure always occurs over an area of the cylinder and not at some particular station between transverse bulkheads. It will be further noted from figure 5 that the bending stress varies linearly between bulkheads. Thus, instead of plotting the bending stress at failure against $\frac{M}{rV}$ as calculated at only one station, it is desirable to plot these values for all stations along the length of the cylinder. This method amounts to plotting the bending-stress diagram with $\frac{M}{rV}$ as the abscissa scale.

On figure 6 are plotted bending-stress diagrams for each test cylinder with ordinates of stress f_b divided by the modulus of elasticity. An inspection of this figure, together with the photographs of the types of failure (figs. 2, 3, and 4), reveals a transition from a shear type of failure at small values of $\frac{M}{rV}$ to a bending type of failure at large values of $\frac{M}{rV}$. In the following discussion separate consideration will be given to bending failure, shear failure, and the transition from bending to shear failure.

Bending failure (large values of $\frac{M}{rV}$).- At large values of $\frac{M}{rV}$ failure occurs by a sudden collapse of the outermost compression fibers in the same manner as in the pure-bending tests reported in reference 3. (See figs. 2 and 4.) It is therefore reasonable to suppose that at these values the bending strength of a thin-walled cylinder should approach the strength of a cylinder of the same dimensions in pure bending.

For comparison of the present results with the results of the pure-bending tests reported in reference 3, lines a and b have been drawn on figure 6 representing the upper and lower limits of the strength in pure bending. These limiting values represent the dispersion of the results of the pure-bending tests and were obtained for cylinders of the average radius/thickness ratio in each group by interpolation of the results plotted in figure 5 of reference 3.

Upon reference to figure 6 it will be noted that, in general, the bending-stress diagrams plot between lines a and b at large values of $\frac{M}{rV}$. Since slight imperfections in the cylinders cause wide variations in the bending strength (reference 3), the few diagrams that plot outside the band established by lines a and b probably represent cylinders in which the imperfections were greater or less than those of the cylinders tested in pure bending.

Shear failure (small values of $\frac{M}{rV}$).- At small values of $\frac{M}{rV}$ failure occurs in shear by the formation of diagonal shear wrinkles on the sides of the cylinders. (See figs. 2 and 3.) It is therefore reasonable to suppose that at these values the shear strength of a thin-walled cylinder should be closely related to the strength of a cylinder of the same dimensions in torsion (pure shear).

For comparison of the present results with the results of the torsion tests reported in reference 1, lines c and d have been drawn on figure 6 representing the probable upper and lower limits for shear failure. These lines were obtained by plotting the equation

$$\frac{f_b}{E} = \frac{S_s}{E} \frac{M}{rV} \tag{4}$$

Equation (4) is obtained from equation (3) by transposing terms, dividing by E, and substituting S_s for f_v, where S_s is the shearing stress at failure for a thin-walled cylinder of the same dimensions in torsion (pure shear, reference 1 or 4). Thus, the value of $\frac{f_b}{E}$ as given by equation (4) is the critical compressive strain on the extreme fiber when failure occurs in shear, provided that the shearing stress at the neutral axis when failure occurs is the same as the shearing stress at failure for a cylinder of the same dimensions in torsion. The lines c and d for shear failure in figure 6 are shown for the two values of S_s calculated as outlined in reference 1 for the largest and smallest radius/thickness ratio for each group of cylinders.

Inspection of figure 6 shows that in some cases the bending-stress diagrams at very low values of $\frac{M}{rV}$, corresponding to shear failure, plot above lines c and d. This fact indicates that the transverse shearing stress on the neutral axis at failure is higher than the shearing stress at failure in torsion. In order to obtain the quantitative relation existing between the two values, $\frac{f_v}{S_s}$ is plotted against $\frac{M}{rV}$ in figure 7 for each of the tests. It is seen then that as $\frac{M}{rV} \rightarrow 0$ the ratio $\frac{f_v}{S_s}$ approaches a value between 1.20 and 1.38. Thus, if S_v is the shearing stress on the neutral axis at failure in pure transverse shear and S_s is the shearing stress at failure for a cylinder of the same dimensions in torsion, S_v and S_s may be related by the following approximate equation

$$S_v = 1.25\ S_s \tag{5}$$

Transition from shear to bending failure (intermediate values of $\frac{M}{rV}$).- It can be seen by reference to figure 6 and figures 2, 3, and 4 that the transition from shear to bending failure is not always as abrupt as the intersection of lines a and b with lines c and d might indicate. At the intermediate values of $\frac{M}{rV}$ the transition from failure by shear to failure by bending is accompanied by a slight reduction in strength. (See groups 3, 4, and 5 of fig. 6 in particular.) The following discussion is offered as a possible explanation of the transition.

When an elastic body is subjected to one type of loading such as torsion, pure bending, compression, or any other loading, it has in general a definite resistance to that loading at which elastic failure occurs and this resistance is ordinarily different for each type of loading. If such a body should be subjected to two or more different types of loading simultaneously, it cannot offer as great a resistance to either type of loading as if that type of loading were acting alone. In such a case the following approximation may be used:

$$\frac{f_1}{S_1} + \frac{f_2}{S_2} + \ldots\ldots \frac{f_n}{S_n} = 1 \tag{6}$$

where S_1, S_2, ... S_n are the critical stress values for different types of loading acting alone on the body, and f_1, f_2, ... f_n are the allowable stress values for those same types of loading when acting simultaneously.

Since a cylinder under combined transverse shear and bending has varying stress conditions around its periphery, the application of equation (6) is made in the following manner. The bending stress at any point θ degrees above the neutral axis is

$$f_b = \frac{M_r \sin\theta}{\pi r^3 t} = \frac{M}{\pi r^2 t} \sin\theta \tag{7}$$

The longitudinal shearing stress at this same point is

$$f_v = \frac{V\ 2t\ r^2 \cos\theta}{2t} = \frac{V \cos\theta}{\pi r t} \tag{8}$$

It is very probable that certain elements of the cylinder reach a critical state of stress before others and that these latter then take a greater proportional share of the load. It is assumed, however, that collapse of the cylinder occurs when all elements have reached such stress conditions that for some fiber the following equation holds

$$\frac{f_v}{S_v} + \frac{f_b}{S_b} = 1 \tag{9}$$

Because of the variation of stress around the periphery

$$\frac{f_v}{S_v} + \frac{f_b}{S_b} = U = f(\theta) \tag{10}$$

The location in the cylinder of the element θ_m for which U is a maximum is obtained by setting the derivative equal to zero. Thus, substitution of the values for f_v

and f_b given by equations (7) and (8) in equation (10) gives

$$U = \frac{M \sin\theta}{\pi r^2 t S_b} + \frac{V \cos\theta}{\pi r t S_v} \tag{11}$$

and the derivative is

$$\frac{dU}{d\theta} = \frac{M \cos\theta}{\pi r^2 t S_b} - \frac{V \sin\theta}{\pi r t S_v} = 0$$

from which

$$\theta_m = \tan^{-1} \frac{M}{rV} \frac{S_v}{S_b} \tag{12}$$

Failure is assumed to occur when $U = 1$ for the element θ_m degrees from the neutral axis on the compression side of the cylinder. With these substitutions, equation (11) becomes

$$1 = \frac{M \sin\theta_m}{\pi r^2 t S_b} + \frac{V \cos\theta_m}{\pi r t S_v} \tag{13}$$

The solution of this equation for M and V, remembering that

$$\tan\theta_m = \frac{M}{rV} \frac{S_v}{S_b}$$

gives

$$M = \pi r^2 t S_b \sin\theta_m \tag{14}$$

$$V = \pi r t S_v \cos\theta_m \tag{15}$$

The strength of a cylinder in pure bending and pure transverse shear is, respectively

$$M = \pi r^2 t S_b \tag{16}$$

$$V = \pi r t S_v \tag{17}$$

Since $\sin\theta_m$ and $\cos\theta_m$ can never exceed unity, equations (14) and (15) show that the presence of shear reduces the bending strength and, conversely, that the pres-

ence of bending reduces the strength in shear. Because equations (14) and (15) are related, both having been derived from equation (13), only one of them need be used to measure the strength of a cylinder in combined transverse shear and bending.

In order to show the effect of shear upon bending in the most effective manner, it is desirable to express the strength of a cylinder under combined transverse shear and bending as a percentage of the strength in pure bending. The curves of figure 8, derived from equations (14) and (16), show this relation as a function of the ratios $\frac{M}{rV}$ and $\frac{S_b}{S_v}$.

In figure 6 the full-curved lines were obtained from figure 8, using in one case the value of $\frac{S_b}{S_v}$ corresponding to lines a and c, and in the other case the value of $\frac{S_b}{S_v}$ corresponding to lines b and d. An inspection of the figures indicates that these two curves represent quite well the limits of the experimental data plotted.

In order to use the curves of figure 8 in design, it is necessary to know the loading condition $\frac{M}{rV}$ and to be able to predict the values of S_b and S_v for the cylinder. If these three quantities are known, the maximum allowable moment and/or stress on the extreme fiber can be read from the chart as a percentage of that for pure bending. The strength in shear then need not be investigated because its effect has been taken into account by a reduced bending strength.

When checking the strength of any section between adjacent bulkheads, the largest value of $\frac{M}{rV}$ in that section should be used to enter the chart of figure 8. This procedure tends toward conservatism and is certainly justified by the wide scattering of the test data.

Wrinkles.- In the preceding paragraphs it has been shown that the strength of a thin-walled cylinder in combined transverse shear and bending can be correlated with the strength of a cylinder of the same dimensions in tor-

sion and pure bending, depending upon whether $\frac{M}{rV}$ is small or large, respectively. It would therefore appear that the size of the shear wrinkles that form on the sides of the cylinder and the bending wrinkles that form near the extreme fiber on the compression half of the cylinder would be the same size, respectively, as the wrinkles for torsion and pure bending. Consequently, experimental values of k, as defined by the equation

$$k = \frac{2\pi r}{\lambda_c}$$

where λ_c is the wave length of a wrinkle in the direction of the circumference, are compared with the corresponding values of k for torsion and pure bending. From table II, where the comparison is made, it will be noted that values of k as calculated for the shear and bending wrinkles compare very well with those tabulated for cylinders of corresponding dimensions in torsion and pure bending, respectively.

CONCLUSIONS

1. For large values of $\frac{M}{rV}$ failure occurred in bending by a sudden collapse of the compression half of the cylinder. The stress on the extreme fiber as calculated by the ordinary beam theory and the size of the wrinkles that formed were both equal to their respective values for a cylinder of the same dimensions in pure bending.

2. For small values of $\frac{M}{rV}$ failure occurred in shear by the formation of diagonal wrinkles on the side of the cylinder. The size and form of the wrinkles at failure were the same as those that occurred at failure for a cylinder of the same dimensions in torsion (pure shear). As $\frac{M}{rV}$ approached zero, the shearing stress on the neutral axis at failure as calculated by the ordinary beam theory was approximately 1.25 times the allowable shearing stress in torsion.

3. At intermediate values of $\frac{M}{rV}$ there was a transition from failure by bending to failure by shear that was

accompanied by a reduction in strength. For use in calculating the strength of thin-walled cylinders in combined transverse shear and bending, a chart is presented that allows for this reduction in strength.

Langley Memorial Aeronautical Laboratory,
National Advisory Committee for Aeronautics
Langley Field, Va., March 4, 1935.

REFERENCES

1. Lundquist, Eugene E.: Strength Tests on Thin-Walled Duralumin Cylinders in Torsion. T.N. No. 427, N.A.C.A., 1932.

2. Lundquist, Eugene E.: Strength Tests of Thin-Walled Duralumin Cylinders in Compression. T.R. No. 473, N.A.C.A., 1933.

3. Lundquist, Eugene E.: Strength Tests of Thin-Walled Duralumin Cylinders in Pure Bending. T.N. No. 479, N.A.C.A., 1933.

4. Donnell, L. H.: Stability of Thin-Walled Tubes Under Torsion. T.R. No. 479, N.A.C.A., 1933.

TABLE I

RESULTS OF COMBINED TRANSVERSE SHEAR AND BENDING TESTS

For all cylinders, $E = 10.4 \times 10^6$ lb. per sq.in. Tabulated values of f_b, f_b/E, and M/rV, taken at bulkhead supported on column. (See fig. 1.)

Group 1 $r = 7.5$ in. $l/r = 1.0$

Spec. No.	t	$\frac{r}{t}$	V	M	f_v	f_b	$\frac{M}{rV}$	$\frac{f_b}{E}$	Remarks
	in.		lb.	lb.-in.	lb./sq.in.	lb./sq.in.			
177	0.0232	323	3593	27400	6580	6690	1.02	0.000643	Failure
183	.0209	359	2663	40080	5410	10860	2.01	.001045	First wrinkle
			2688	40480	5460	10960	2.01	.001054	Failure
188	.0210	357	2413	46490	4880	12530	2.57	.001205	Failure
184	.0209	359	1753	40540	3560	10980	3.09	.001056	Failure
187	.0208	361	2488	63610	5080	17330	3.41	.001666	Failure
189	.0210	357	1978	50860	4000	13710	3.43	.001318	Failure
185	.0205	366	1268	40070	2630	11060	4.21	.001063	Failure
186	.0208	361	1508	55020	3080	14990	4.87	.001441	Failure
190	.0207	362	1138	42170	2330	11520	4.94	.001107	Failure
191	.0207	362	992	57770	2030	15750	7.76	.001514	Failure

Group 2 $r = 7.5$ in. $l/r = 1.0$

Spec. No.	t	$\frac{r}{t}$	V	M	f_v	f_b	$\frac{M}{rV}$	$\frac{f_b}{E}$	Remarks
	in.		lb.	lb.-in.	lb./sq.in.	lb./sq.in.			
176	0.0166	452	1413	10520	3615	3580	0.99	0.000370	First wrinkle
			1723	12920	4410	4400	1.00	.000423	Failure
175	.0156	481	1533	11450	4160	4150	1.00	.000399	First wrinkle
			1593	11910	4330	4320	1.00	.000415	Failure
161	.0164	457	1378	20830	3570	7180	2.02	.000690	First wrinkle
			1398	21130	3620	7290	2.02	.000701	Failure
178	.0157	478	1033	16270	2790	5850	2.10	.000562	First wrinkle
			1103	17330	2980	6230	2.09	.000599	Failure
182	.0159	472	1148	22140	3060	7880	2.57	.000758	Failure
180	.0157	478	1128	24910	3050	8970	2.94	.000862	Failure
179	.0153	490	708	23270	1960	8580	4.38	.000825	Failure
173	.0155	484	381	25060	1045	9150	8.78	.000879	Failure
174	.0157	478	273	19250	737	6925	9.40	.000666	Failure

TABLE I (Cont.)

Group 3 r = 7.5 in. l/r = 0.5

Spec. No.	t	$\frac{r}{t}$	V	M	f_v	f_b	$\frac{M}{rV}$	$\frac{f_b}{E}$	Remarks
	in.		lb.	lb.-in.	lb./sq.in.	lb./sq.in.			
111	0.0121	620	843	5360	2960	2510	0.85	0.000241	First wrinkle
			1143	7310	4010	3420	.85	.000329	Failure
78	.0115	652	663	7260	2445	3580	1.46	.000344	First wrinkle
			928	10100	3425	4970	1.45	.000478	Failure
1	.0112	670	843	9710	3195	4905	1.54	.000472	First wrinkle
			905	10400	3430	5250	1.53	.000505	Failure
114	.0117	641	568	8800	2060	4250	2.07	.000409	First wrinkle
			653	10040	2365	4850	2.05	.000466	Failure
110	.0120	625	703	10780	2480	5080	2.05	.000489	First wrinkle
			753	11500	2660	5420	2.04	.000521	Failure
108	.0119	630	588	9100	2100	4330	2.06	.000416	First wrinkle
			688	10550	2460	5020	2.04	.000483	Failure
76	.0113	663	753	11500	2830	5750	2.04	.000553	Failure
113	.0116	646	658	10130	2410	4940	2.05	.000475	Failure
107	.0118	635	668	13030	2400	6230	2.60	.000601	First wrinkle
			738	14290	2655	6840	2.58	.000657	Failure
104	.0114	658	488	9790	1815	4850	2.67	.000466	First wrinkle
			628	12310	2335	6090	2.61	.000586	Failure
77	.0114	658	663	13140	2465	6500	2.64	.000625	First wrinkle
			678	13420	2520	6640	2.64	.000638	Failure
106	.0116	646	563	13530	2060	6600	3.20	.000634	Failure
94	.0128	586	513	18460	1700	8160	4.80	.000786	Failure
97	.0121	620	413	15360	1450	7180	4.96	.000690	Failure
105	.0116	646	358	13660	1310	6660	5.09	.000640	Failure
95	.0119	630	413	17990	1475	8570	5.81	.000824	Failure
101	.0116	646	338	15670	1237	7640	6.18	.000734	Failure
96	.0120	625	318	15050	1125	7100	6.31	.000682	Failure
103	.0120	625	308	14740	1090	6950	6.38	.000668	Failure

Group 4 r = 7.5 in. l/r = 1.0

Spec. No.	t	$\frac{r}{t}$	V	M	f_v	f_b	$\frac{M}{rV}$	$\frac{f_b}{E}$	Remarks
	in.		lb.	lb.-in.	lb./sq.in.	lb./sq.in.			
15	0.0110	682	579	4570	2235	2355	1.05	0.000226	First wrinkle
			696	5570	2690	2870	1.07	.000276	Failure
85	.0114	658	529	4150	1975	2055	1.05	.000197	First wrinkle
			722	5790	2680	2870	1.07	.000276	Failure
11	.0111	675	586	7130	2240	3640	1.62	.000350	First wrinkle
			666	8070	2540	4120	1.62	.000396	Failure
87	.0110	682	474	5810	1830	2980	1.63	.000287	First wrinkle
			599	7370	2310	3780	1.64	.000363	Failure
83	.0115	652	544	6680	2010	3290	1.64	.000316	First wrinkle
			609	7490	2245	3690	1.64	.000355	Failure
81	.0115	652	519	8920	1915	4390	2.29	.000422	First wrinkle
			581	9940	2145	4900	2.28	.000471	Failure
12	.0112	669	475	8340	1800	4210	2.34	.000405	First wrinkle
			575	10010	2180	5050	2.32	.000485	Failure
75	.0113	663	474	9070	1780	4535	2.55	.000436	First wrinkle
			504	9610	1895	4805	2.54	.000462	Failure
31	.0111	675	472	9225	1810	4710	2.61	.000453	Failure
74	.0114	658	388	8800	1440	4350	3.02	.000418	First wrinkle
			458	10240	1700	5070	2.98	.000487	Failure
73	.0112	669	453	10140	1715	5120	2.98	.000492	Failure
13	.0108	694	395	9280	1550	4860	3.13	.000467	First wrinkle
			400	9380	1570	4910	3.13	.000472	Failure
92	.0114	658	433	11950	1610	5920	3.68	.000569	Failure
91	.0112	669	393	10970	1490	5540	3.72	.000533	Failure
89	.0112	669	329	9390	1245	4740	3.81	.000456	Failure
72	.0116	646	378	13330	1385	6500	4.70	.000625	Failure
71	.0117	641	378	13330	1370	6440	4.70	.000619	Failure
16	.0110	682	375	13350	1450	6880	4.75	.000661	Failure
69	.0119	630	308	15770	1095	7470	6.83	.000722	Failure
70	.0119	630	298	15420	1060	7310	6.90	.000706	Failure
14	.0108	694	186	11830	730	6190	8.48	.000595	Failure
112	.0120	625	157	15090	555	7120	12.83	.000684	Failure
93	.0115	652	152	14790	560	7280	13.00	.000700	Failure
37	.0118	635	126	13500	453	6480	14.28	.000620	Failure

TABLE I (Cont.)

Group 5 r = 7.5 in. l/r = 2.0

Spec. No.	t	$\frac{r}{t}$	V	M	f_v	f_b	$\frac{M}{rV}$	$\frac{f_b}{E}$	Remarks
	in.		lb.	lb.-in.	lb./sq.in.	lb./sq.in.			
65	0.0114	658	314	3170	1170	1576	1.35	0.000151	First wrinkle
			506	5570	1880	2770	1.47	.000265	Failure
17	.0111	676	410	4590	1570	2340	1.49	.000225	First wrinkle
			510	5890	1950	3010	1.54	.000289	Failure
100	.0115	652	463	6790	1710	3350	1.96	.000322	First wrinkle
			503	7400	1860	3650	1.96	.000351	Failure
18	.0111	675	455	6640	1740	3390	1.95	.000326	First wrinkle
			510	7480	1950	3820	1.96	.000367	Failure
29	.0113	664	537	11560	2020	5780	2.87	.000556	Failure
67	.0120	625	479	10350	1695	4880	2.88	.000469	First wrinkle
			491	10610	1740	5010	2.88	.000481	Failure
19	.0110	682	395	8590	1525	4430	2.90	.000426	First wrinkle
			410	8900	1580	4580	2.90	.000440	Failure
99	.0120	625	444	11570	1570	5460	3.47	.000525	First wrinkle
			469	12195	1660	5750	3.46	.000553	Failure
98	.0120	625	419	10950	1480	5160	3.49	.000496	First wrinkle
			464	12070	1640	5690	3.47	.000547	Failure
64	.0116	646	361	11890	1320	5800	4.39	.000557	Failure
20	.0116	647	385	12690	1405	6190	4.40	.000595	Failure
66	.0129	581	509	16950	1675	7440	4.44	.000714	Failure
65	.0114	658	209	9740	1080	4850	4.49	.000463	Failure
63	.0111	675	249	12400	954	6330	6.64	.000608	Failure
21	.0109	688	260	12990	1010	6730	6.66	.000646	Failure
62	.0117	641	220	14360	797	6940	8.70	.000667	Failure
61	.0117	641	210	13940	760	6740	8.86	.000647	Failure
22	.0114	658	205	13870	765	6900	9.02	.000660	Failure

TABLE I (Cont.)

Group 6 r = 15 in. l/r = 1.0

Spec. No.	t	$\frac{r}{t}$	V	M	f_v	f_b	$\frac{M}{rV}$	$\frac{f_b}{E}$	Remarks
	in.		lb.	lb.-in.	lb./sq.in.	lb./sq.in.			
224	0.0206	728	2315	36550	2386	2510	1.05	0.000241	Failure
223	.0221	679	2375	53000	2280	3390	1.49	.000326	Failure
228	.0224	670	2145	66800	2030	4220	2.08	.000406	Failure
226	.0213	704	1885	59000	1880	3920	2.09	.000377	Failure
225	.0201	746	1185	57200	1250	4020	3.22	.000387	Failure
227	.0231	649	1485	73100	1365	4470	3.28	.000430	Failure

Group 7 r = 15 in. l/r = 1.0

Spec. No.	t	$\frac{r}{t}$	V	M	f_v	f_b	$\frac{M}{rV}$	$\frac{f_b}{E}$	Remarks
	in.		lb.	lb.-in.	lb./sq.in.	lb./sq.in.			
218	0.0155	968	1065	16630	1457	1518	1.04	0.000146	First wrinkle
			1165	18120	1595	1655	1.04	.000159	Failure
222	.0153	980	825	18890	1145	1747	1.53	.000168	First wrinkle
			1010	22970	1400	2125	1.52	.000204	Failure
219	.0161	932	985	31970	1300	2810	2.16	.000270	Failure
220	.0161	932	765	30870	1008	2710	2.69	.000261	Failure
217	.0161	932	585	30770	770	2700	3.51	.000260	Failure
221	.0158	949	525	30830	705	2760	3.92	.000265	Failure

Group 8 r = 15 in. l/r = 1.0

Spec. No.	t	$\frac{r}{t}$	V	M	f_v	f_b	$\frac{M}{rV}$	$\frac{f_b}{E}$	Remarks
	in.		lb.	lb.-in.	lb./sq.in.	lb./sq.in.			
209	0.0103	1455	405	6800	834	932	1.12	0.0000896	Failure
214	.0111	1352	315	10210	602	1300	2.16	.000125	First wrinkle
			425	13190	812	1680	2.07	.000161	Failure
210	.0116	1293	485	16890	887	2060	2.32	.000198	Failure
213	.0106	1415	335	14600	672	1946	2.90	.000187	Failure
212	.0110	1364	305	15100	588	1940	3.30	.000187	Failure
211	.0110	1364	275	16900	530	2172	4.10	.000209	Failure
216	.0103	1455	125	13225	257	1815	7.06	.000175	Failure
215	.0105	1428	105	12330	212	1660	7.83	.000160	Failure

TABLE II

COMPARISON OF EXPERIMENTAL VALUES OF K FOR BENDING, TORSION,

AND COMBINED TRANSVERSE SHEAR AND BENDING TESTS

(Values of k for torsion tests obtained from fig. 7 of reference 1.
Values of k for pure bending tests obtained from table I of reference 3.)

Radius	$\frac{l}{r}$	t = 0.011 (in.)				t = 0.016 (in.)				t = 0.022 (in.)			
		Torsion (pure shear)	Pure bending	Transverse shear and bending		Torsion (pure shear)	Pure bending	Transverse shear and bending		Torsion (pure shear)	Pure bending	Transverse shear and bending	
				Shear	Bending			Shear	Bending			Shear	Bending
in.													
7.5	0.5	21	15-16	21	13-16								
7.5	1.0	16-17	10-13	16-17	11-13	15	11-12	15	9-14	13-14	10-13	13-14	10-15
7.5	2.0	11-12	9-11	12-13	10-12								
15.0	1.0	18	11-13	17-19	10-14	17	11-12	17-21	11-13	16-17	8-12	16-17	-

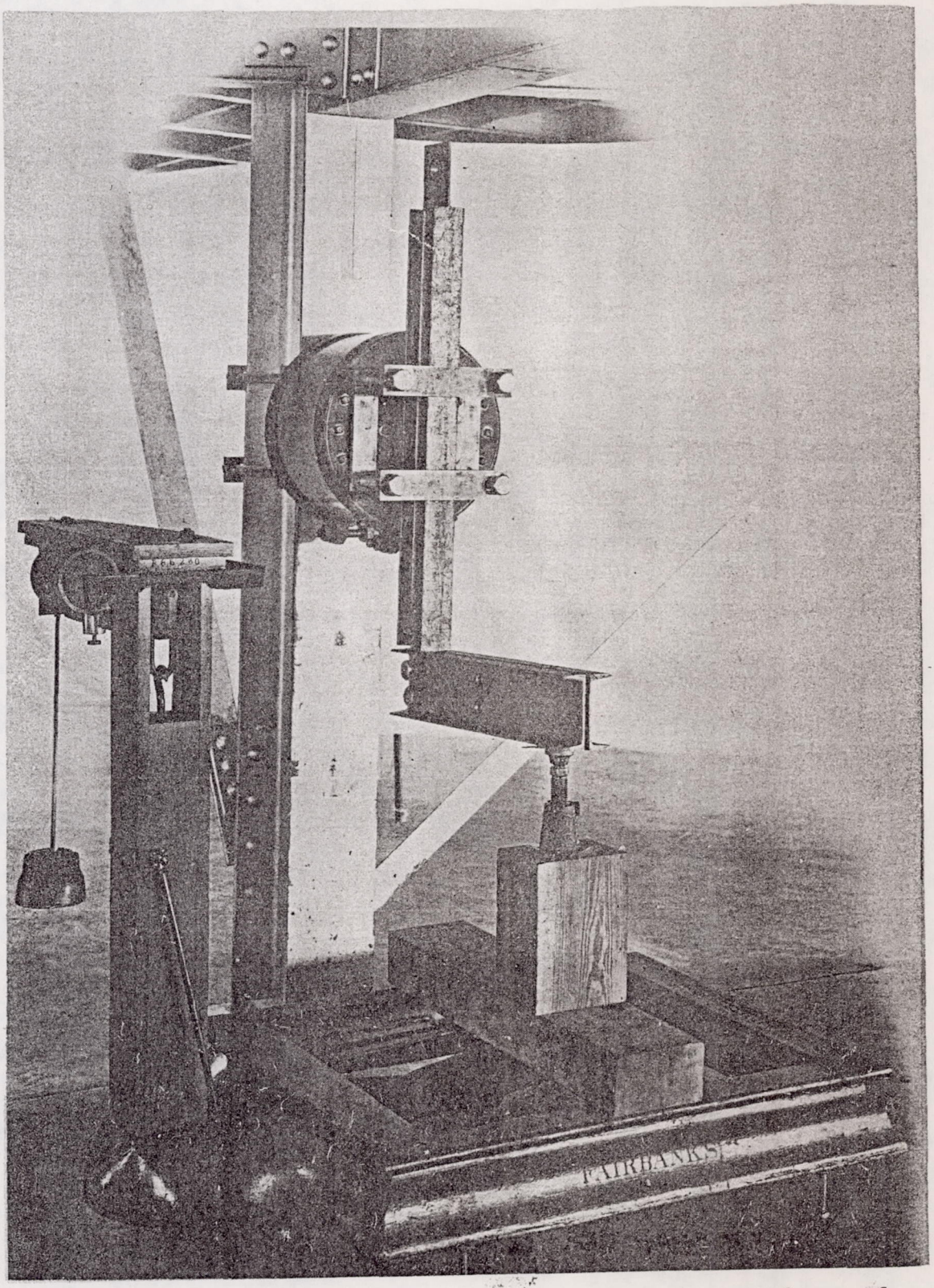

Figure 1.- Loading apparatus used in combined transverse shear and bending tests.

$\frac{M}{rV}$ = -0.53 to 1.47

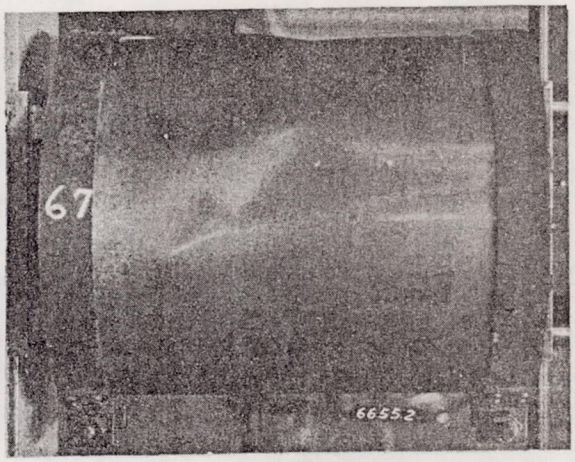

$\frac{M}{rV}$ = 0.88 to 2.88

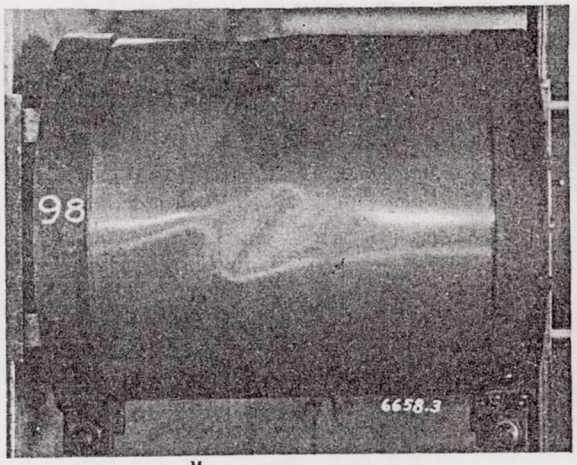

$\frac{M}{rV}$ = 1.47 to 3.47

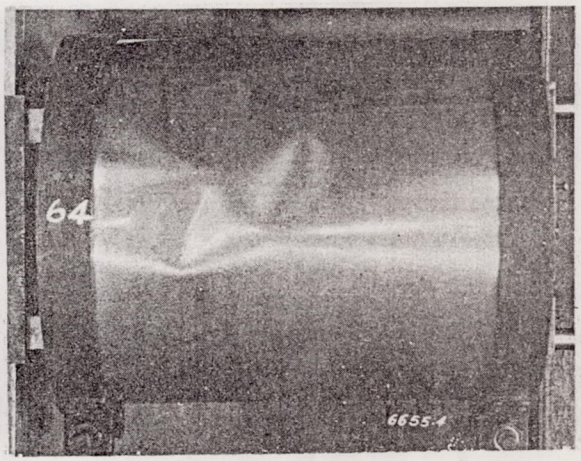

$\frac{M}{rV}$ = 2.39 to 4.39

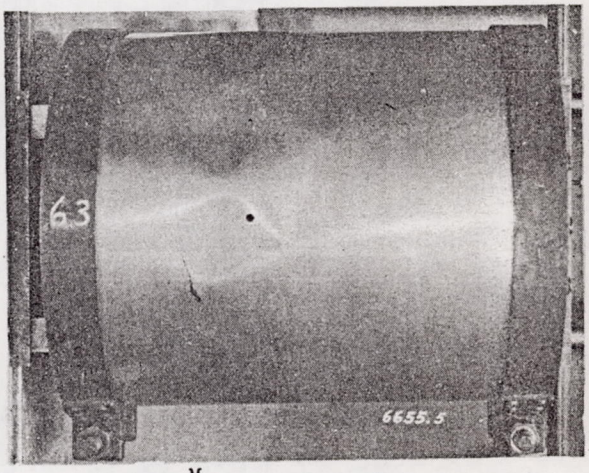

$\frac{M}{rV}$ = 4.64 to 6.64

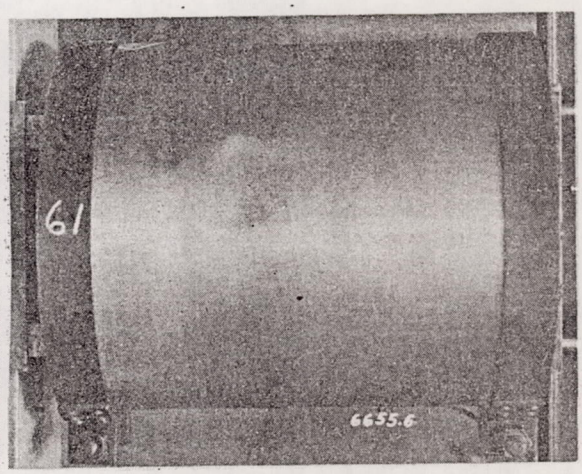

$\frac{M}{rV}$ = 6.85 to 8.85

Figure 2.- Side view of circular cylinders after failure in combined transverse shear and bending tests, cylinders of group 5

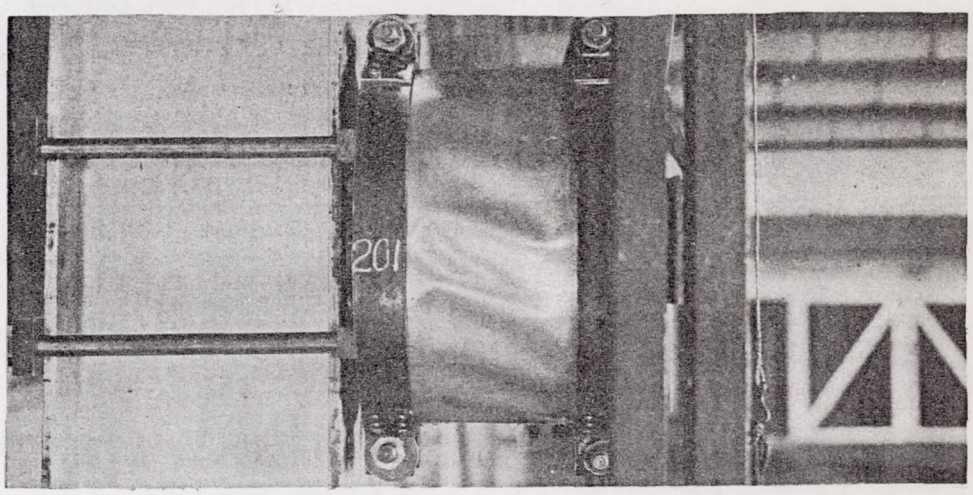

$\frac{l}{r} = 0.87$

$\frac{l}{r} = 2.0$

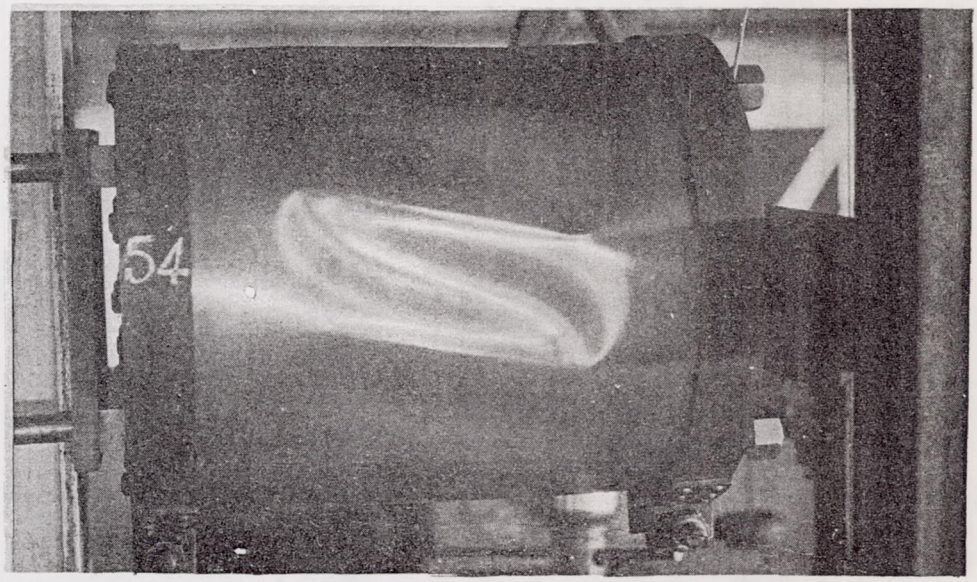

Fig. 3

Cylinders after failure in torsion (fig. 4, reference 1).

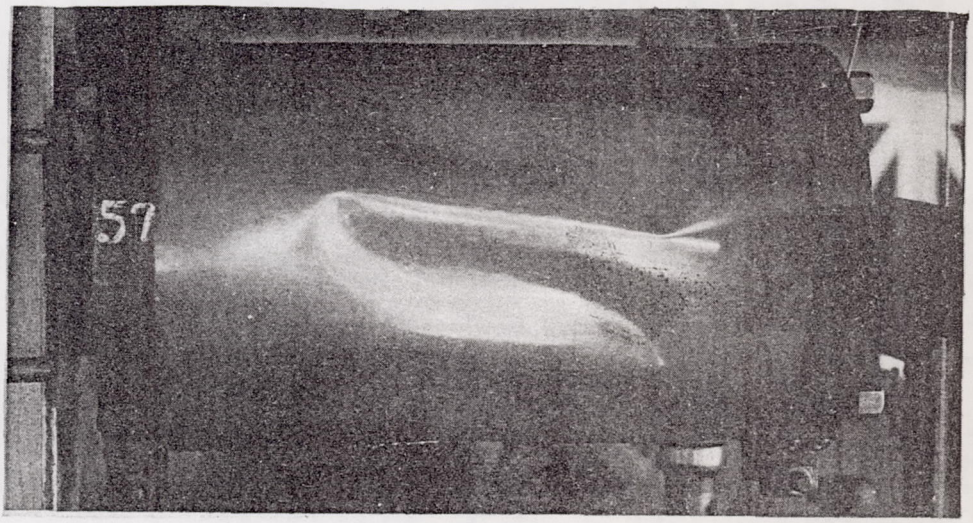

$\frac{l}{r} = 3.0$

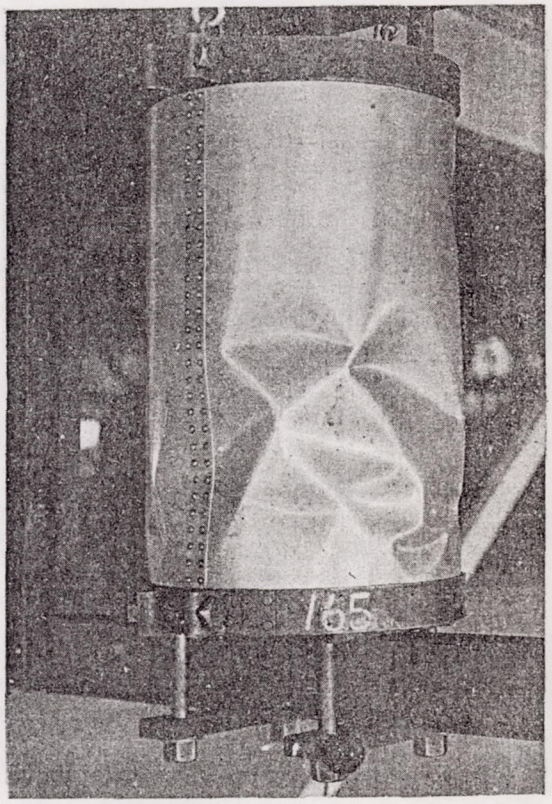

$r = 7.5$ in.; $\frac{l}{r} = 3.00$; $\frac{r}{t} = 346$

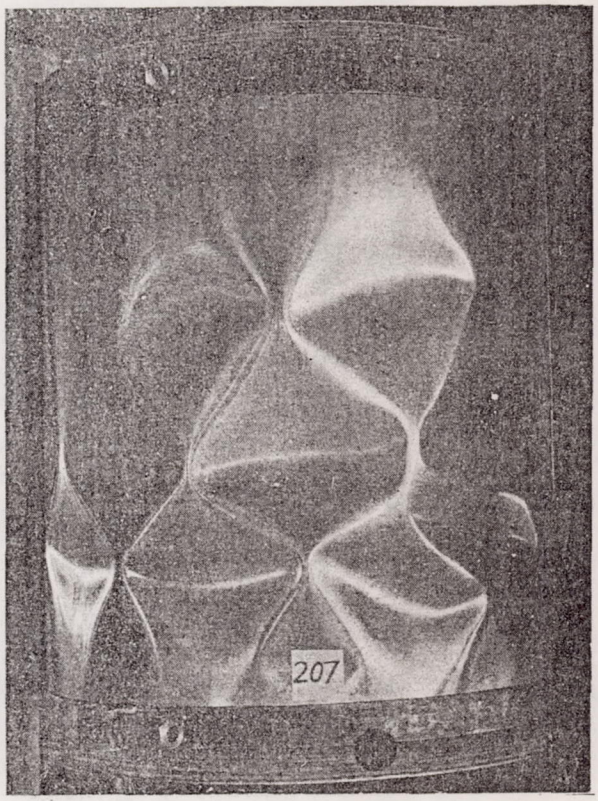

$r = 15.0$ in.; $\frac{l}{r} = 2.00$; $\frac{r}{t} = 673$

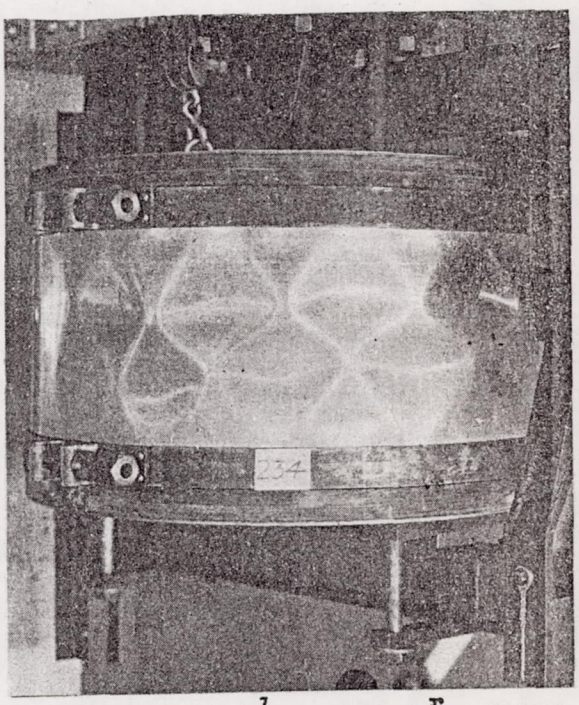

$r = 15.0$ in.; $\frac{l}{r} = 0.70$; $\frac{r}{t} = 980$

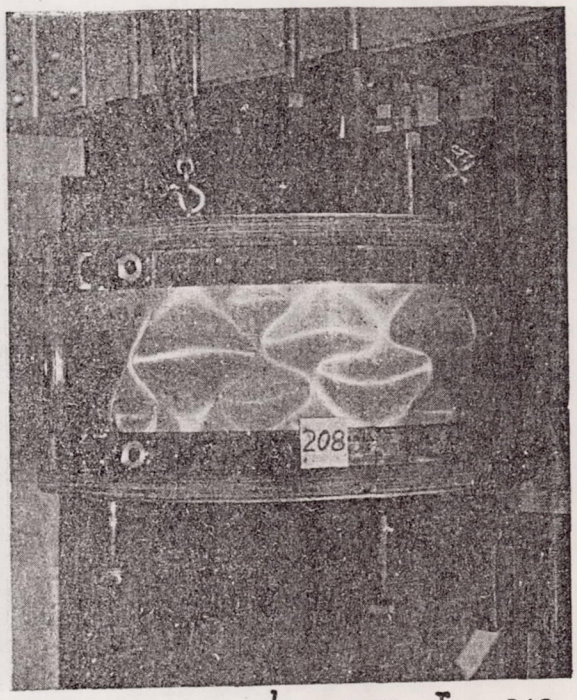

$r = 15.0$ in.; $\frac{l}{r} = 0.50$; $\frac{r}{t} = 949$

Figure 4.- Cylinders after failure in pure bending (fig. 2, reference 3).

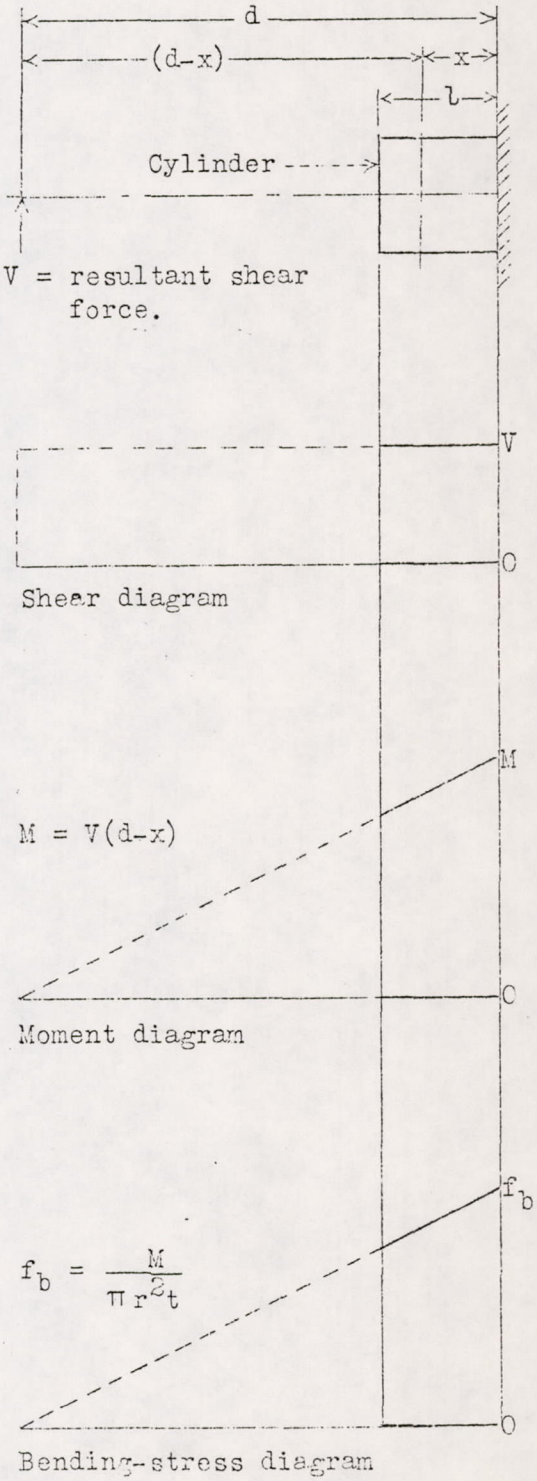

Figure 5.-Shear, moment, and bending-stress diagrams for a cylinder in combined transverse shear and bending.

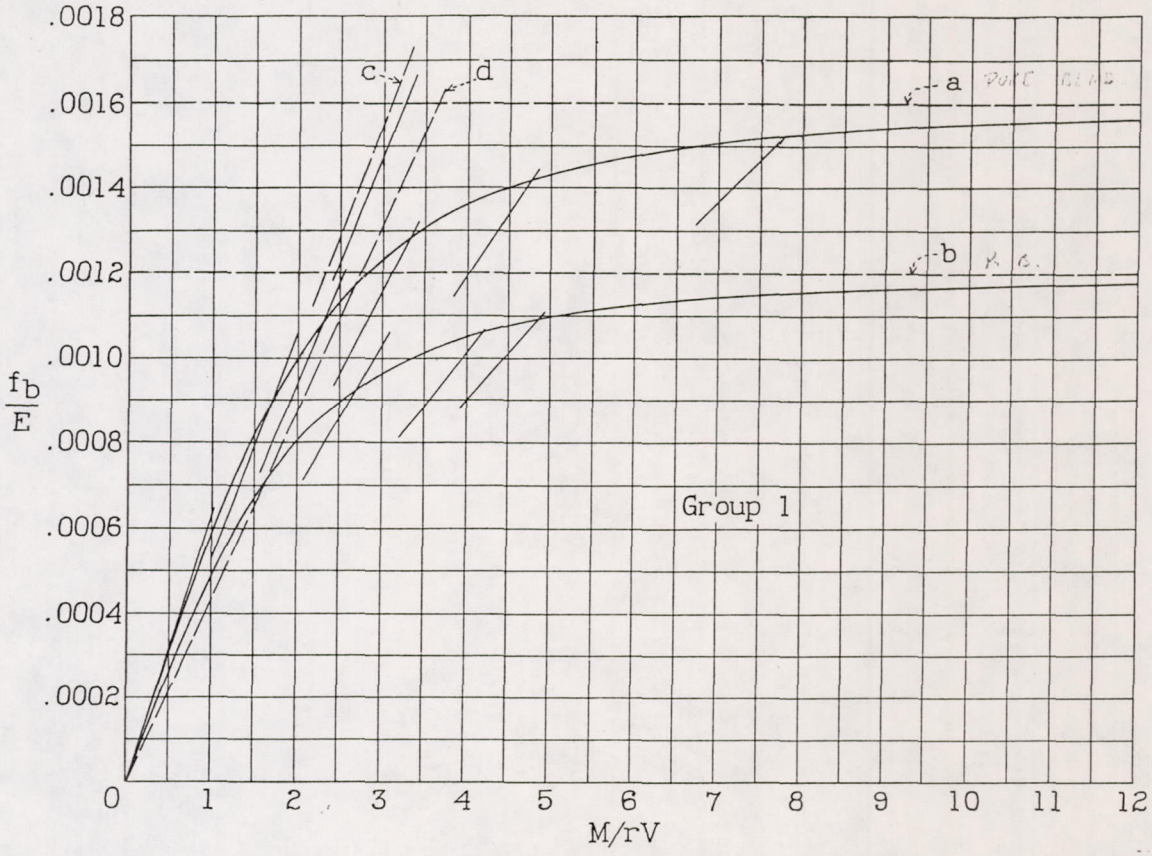

Figure 6a.- Bending-stress diagrams for circular cylinders in combined transverse shear and bending.

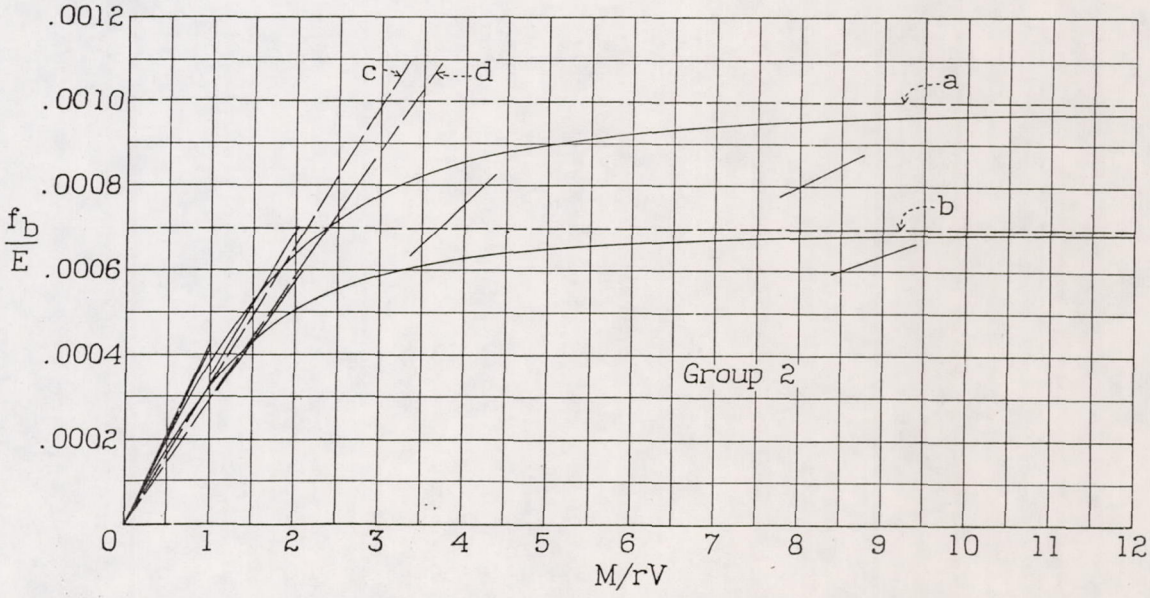

Figure 6b.- Bending-stress diagrams for circular cylinders in combined transverse shear and bending.

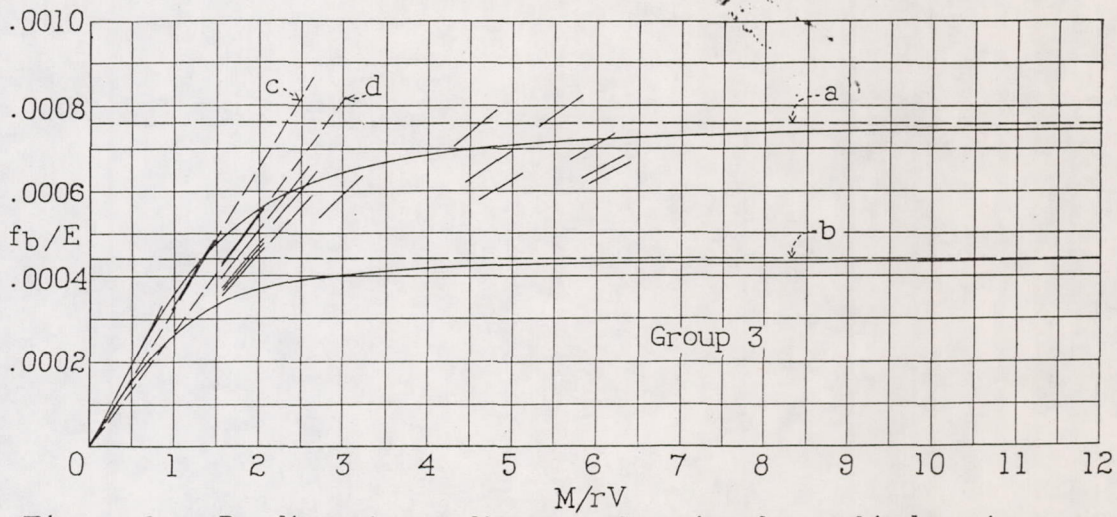

Figure 6c.- Bending-stress diagrams for circular cylinders in combined transverse shear and bending.

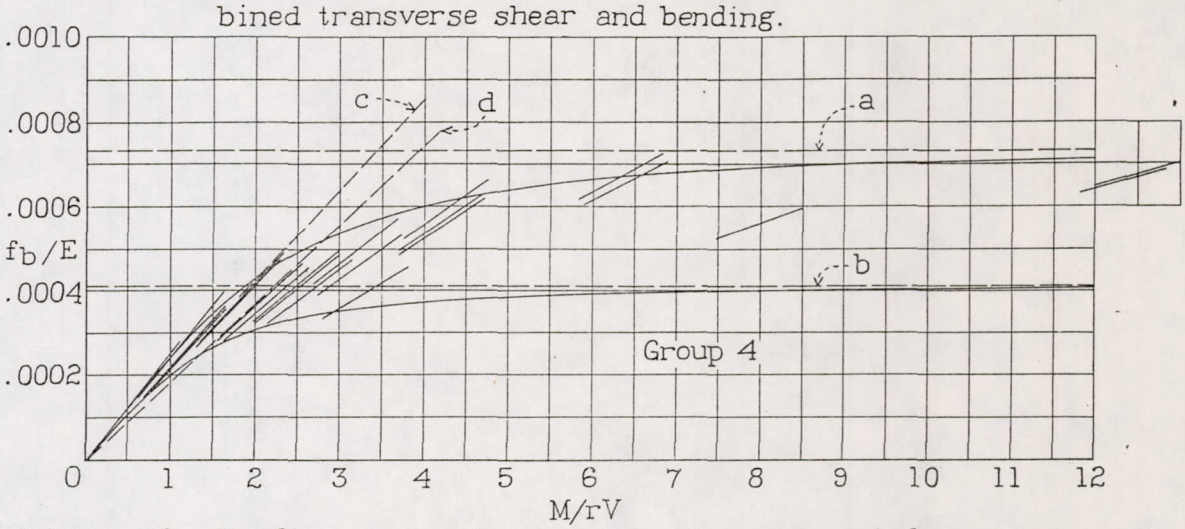

Figure 6d.- Bending-stress diagrams for circular cylinders in combined transverse shear and bending.

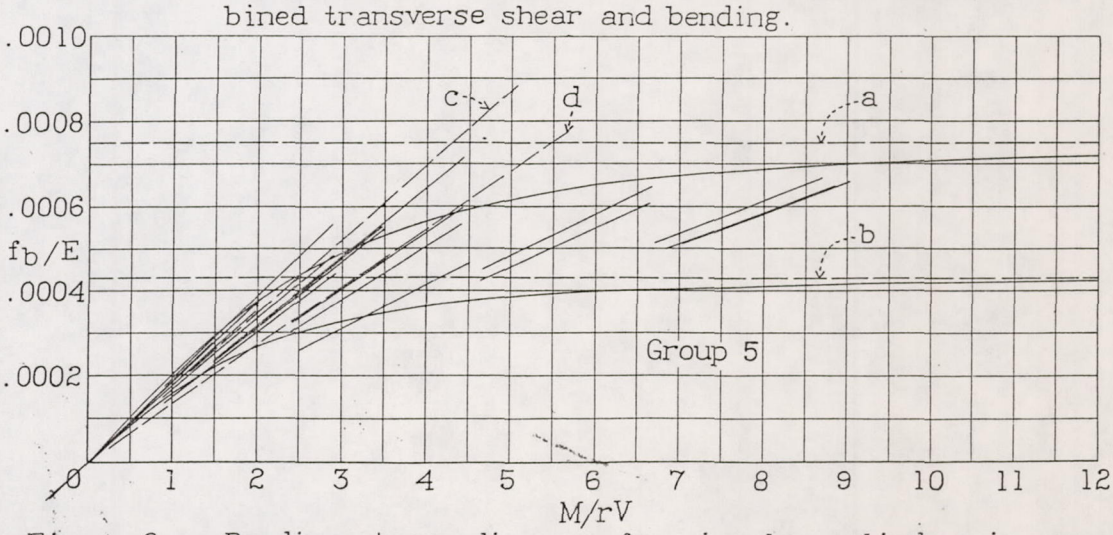

Figure 6e.- Bending-stress diagrams for circular cylinders in combined transverse shear and bending.

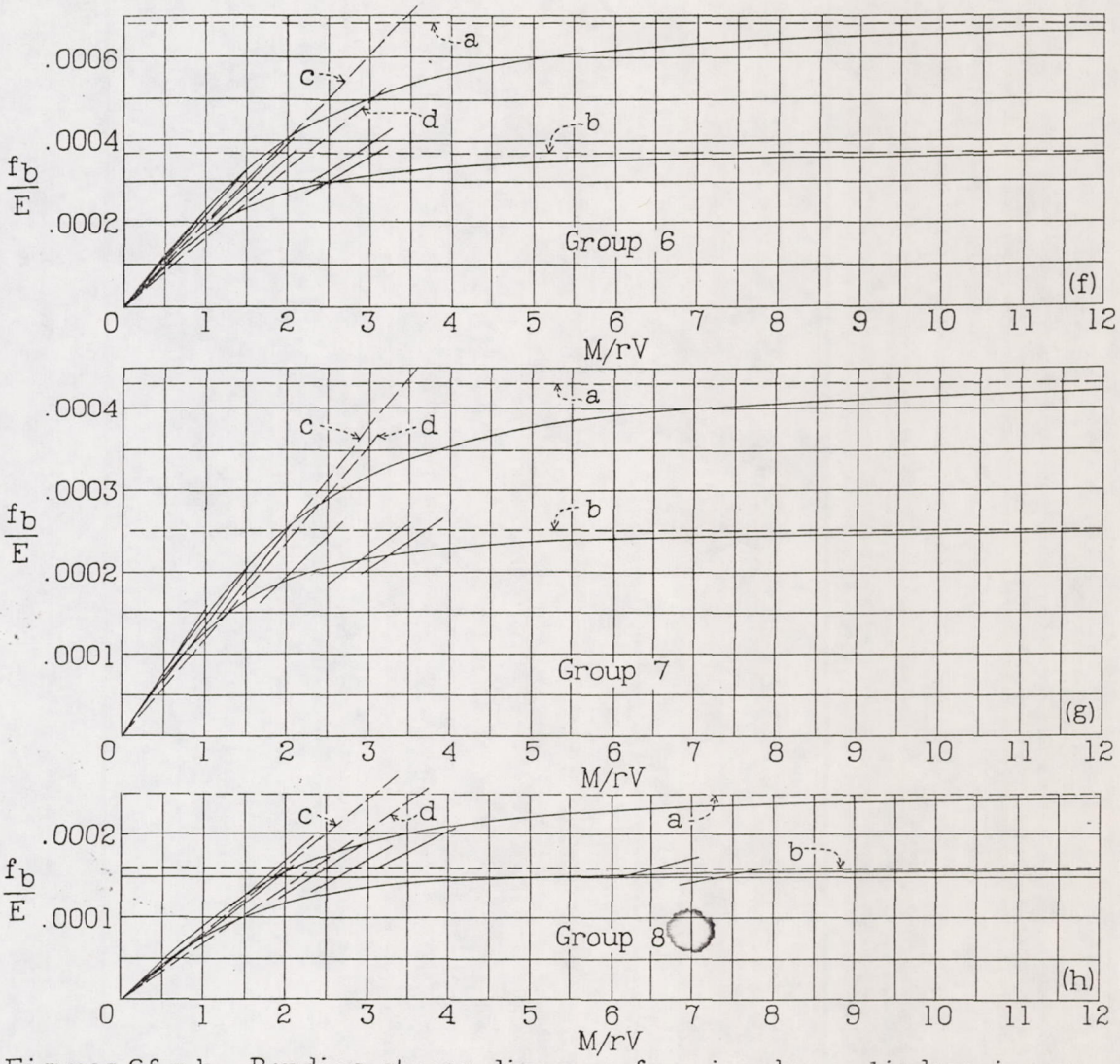

Figures 6f,g,h.- Bending-stress diagrams for circular cylinders in combined transverse shear and bending.

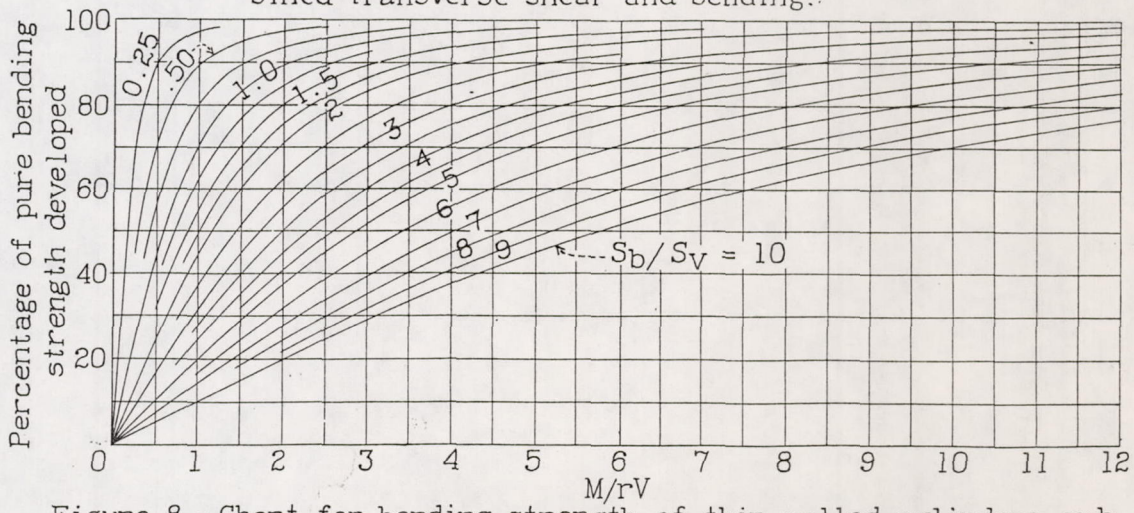

Figure 8.- Chart for bending strength of thin-walled cylinders subjected to combined transverse shear and bending.

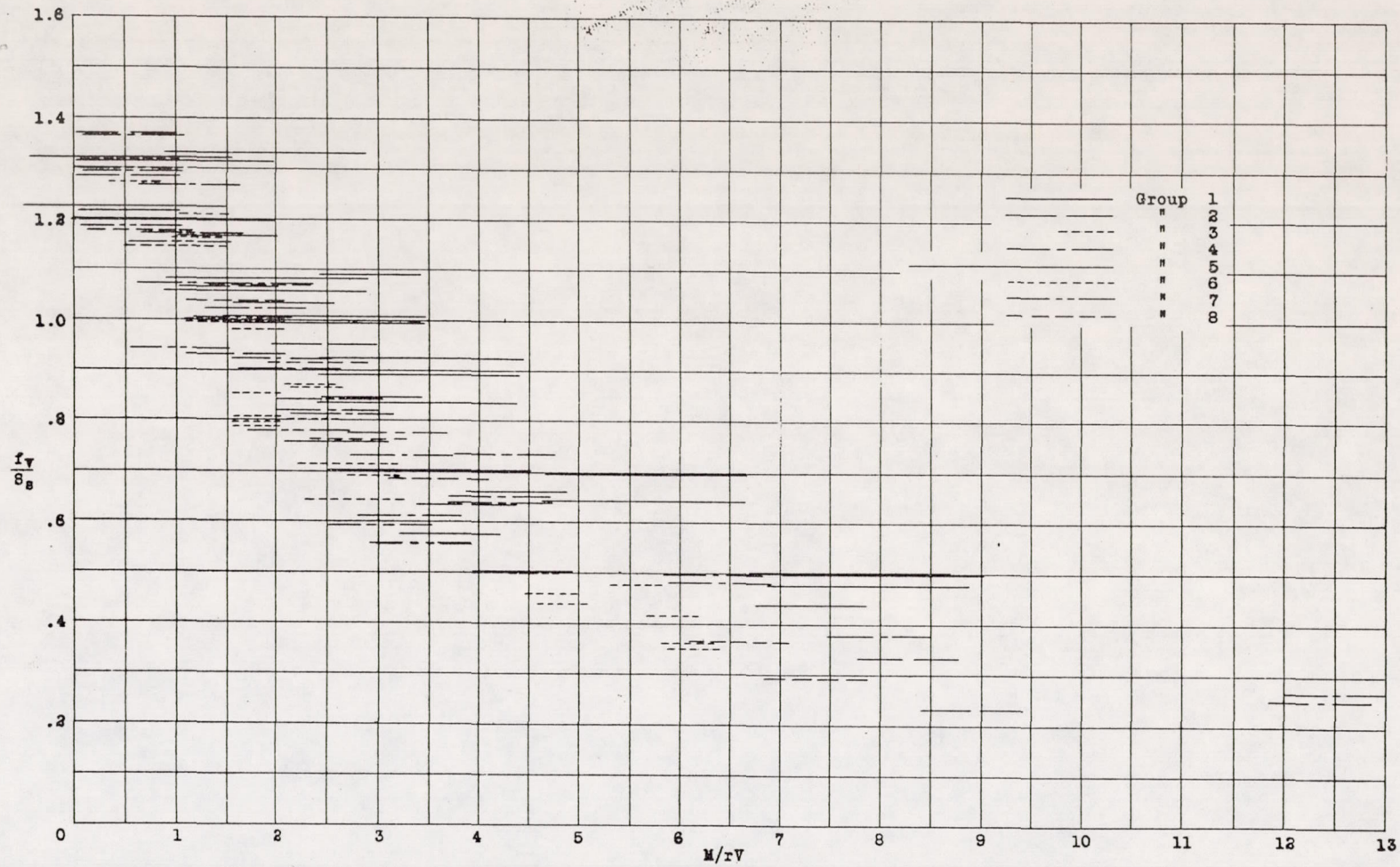

Figure 7.- Shearing-stress diagrams for circular cylinders in combined transverse shear and bending.

U.S. DEPARTMENT OF COMMERCE
National Technical Information Service

NACA-TN-523

STRENGTH TESTS OF THIN-WALLED DURALUMIN CYLINDERS IN COMBINED TRANSVERSE SHEAR AND BENDING

Langley Memorial Aeronautical Laboratory
Washington, DC

Apr 35

29